PAPER

Check for updates

Natural-product-inspired design and synthesis of thiolated coenzyme Q analogs as promising agents against Gram-positive bacterial strains: insights into structure–activity relationship, activity profile, mode of action, and molecular docking†

Hatice Yıldırım, [a] Mahmut Yıldız, [b] Nilüfer Bayrak, [a] Emel Mataracı-Kara, [c] Berna Özbek-Çelik, [c] Masami Otsuka, [de] Mikako Fujita, [d] Mohamed O. Radwan [df] and Amaç Fatih TuYuN [*g]

In an attempt to develop effective and potentially active antibacterial and/or antifungal agents, we designed, synthesized, and characterized thiolated CoQ analogs (**CoQ1–8**) with an extensive antimicrobial study. The antimicrobial profile of these analogs was determined using four Gram-negative bacteria, three Gram-positive bacteria, and three fungi. Because of the fact that the thiolated CoQ analogs were quite effective on all tested Gram-positive bacterial strains, including *Staphylococcus aureus* (ATCC® 29213) and *Enterococcus faecalis* (ATCC® 29212), the first two thiolated CoQ analogs emerged as potentially the most desirable ones in this series. Importantly, after the evaluation of the antibacterial and antifungal activity, we presented an initial structure–activity relationship for these CoQ analogs. In addition, the most promising thiolated CoQ analogs (**CoQ1** and **CoQ2**) having the lowest MIC values on all tested Gram-positive bacterial strains, were further evaluated for their inhibition capacities of biofilm formation after evaluating their *in vitro* potential antimicrobial activity against each of 20 clinically obtained resistant strains of Gram-positive bacteria. **CoQ1** and **CoQ2** exhibited potential molecular interactions with *S. aureus* DNA gyrase in addition to excellent pharmacokinetics and lead-likeness profiles. Our findings offer important implications for a potential antimicrobial drug candidate, in particular for the treatment of infections caused by clinically resistant MRSA isolates.

1. Introduction

1,4-Quinones are important motifs in bioactive molecules that find widespread applications in cancer, microbiology, and material sciences because of two possible main reasons.[1–4] Firstly, the 1,4-quinone core has been historically used as a small template for the preparation of biologically active molecules.[2,4,5] Secondly, it is now well documented that the insertion of amino and/or thio group(s) into the quinone motif can lead to profound contributions to their physical, chemical,

and, in particular, biological properties.[6,7] Accordingly, an increasing number of aminated and/or thiolated quinones have been prepared, leading to the discovery of novel bioactive products.[8–10] Mono- and/or disubstituted quinone motifs, in particular, are present in various pharmacologically related molecules, including those used as lead molecules for Leber's Hereditary Optic Neuropathy (LHON),[11] anticancer,[12] antibacterial,[13,14] antifungal,[15,16] antiHIV,[17] and antimalarial therapy.[18] It is worth noting that some 1,4-quinones have also found use as functional ligands for transition metals.[19–22]

[a]Department of Chemistry, Engineering Faculty, Istanbul University-Cerrahpasa, Avcilar, 34320, Istanbul, Turkey

[b]Department of Chemistry, Gebze Technical University, Gebze, 41400, Kocaeli, Turkey

[c]Department of Pharmaceutical Microbiology, Pharmacy Faculty, Istanbul University, Beyazit, 34116, Istanbul, Turkey

[d]Medicinal and Biological Chemistry Science Farm Joint Research Laboratory, Faculty of Life Sciences, Kumamoto University, 5–1 Oe-honmachi, Chuo-ku, Kumamoto 862–0973, Japan

[e]Department of Drug Discovery, Science Farm Ltd, 1–7–30 Kuhonji, Chuo-ku, Kumamoto 862–0976, Japan

[f]Chemistry of Natural Compounds Department, Pharmaceutical and Drug Industries Research Division, National Research Centre, Dokki, Cairo 12622, Egypt

[g]Department of Chemistry, Faculty of Science, Istanbul University, Fatih, Istanbul, Turkey. E-mail: aftuyun@gmail.com; aftuyun@istanbul.edu.tr; Tel: +90 212 440 0000

† Electronic supplementary information (ESI) available. CCDC 2150434. For ESI and crystallographic data in CIF or other electronic format see https://doi.org/10.1039/d2ra02136f
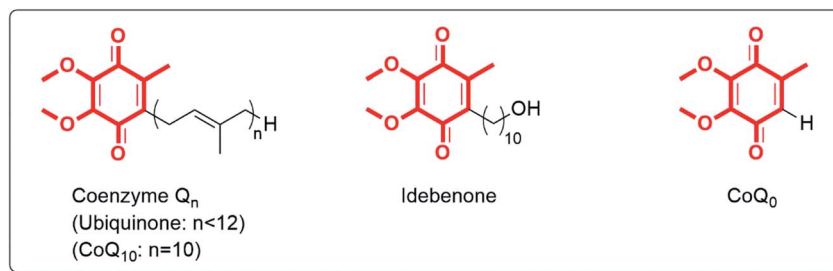
Fig. 1 The most important members of the coenzyme Qn (CoQn) family.

What's more, the Coenzyme Qn (CoQn) family, also named as the ubiquinones, has occupied a unique position in the design and synthesis of novel biologically active lead molecules that exert remarkable medicinal activity.[23] Besides of versatile properties, not surprisingly, ubiquinone participating in the cellular aerobic respiration process,[24] plastoquinone and phylloquinone serving as electron acceptors in electron transport chains in photosynthesis, and vitamin K participating coagulation process and preventing bleeding have also a 1,4-quinone motif.[25,26] To date, some important molecules such as idebenone and **CoQ10** have been under clinical investigation (Fig. 1).[27,28] Of these, idebenone is the only drug in the treatment of emotional disturbances associated with cerebrovascular diseases developed by Takeda Pharmaceutical Company Ltd to have been approved by the European Medicines Agency (EMA) for only under exceptional circumstances.[29] In addition, CoQ is an important medicine, in particular **CoQ10** which is sold in many countries as a dietary supplement to improve immunotherapy[30] has a valuable efficacy on versatile heart-related diseases, hepatitis, and cancer.[31]

In the past 10 years or so, we have prepared a different series of analogs of some important molecules containing 1,4-quinone core to explore the structure–activity relationships

(SARs) around this motif as shown in Fig. 2.[32] We focused on the insertion of amino (primary or secondary amines) and/or thio (aromatic or alkyl chain thiols) group(s) into the 1,4-quinone motif. On the other hand, by keeping these group(s) within 1,4-quinone moiety, we used the quinone fused with benzene named as naphthoquinone[33,34] or vitamin K analogs, or attached to the dimethyl groups named as plastoquinone analogs,[35–37] or fused with pyridine named as quinolinequinone analogs.[8,38,39] The substituents within the amino and/or thio group(s) and the groups attached to the 1,4-quinone motif for the different series contribute significantly toward biological efficacy.[8] Thus, our studies should be useful to predict which modification of the groups attached to the 1,4-quinone motif could enhance biological potency. These results motivated us to design and synthesize new analogs based on the important structure of **CoQ0** containing a core methyl-1,4-quinone motif mostly similar to vitamin K. Encouraged by our previous results and literature, apart from the synthesis under mild conditions, the target analogs of **CoQ0** was then evaluated for the antimicrobial evaluation to reveal the effect of the modification on their potency. Indeed, the most important members of the **CoQ0** with thiols were investigated for their antibiofilm activity, potential antimicrobial activity against each of 20 clinically
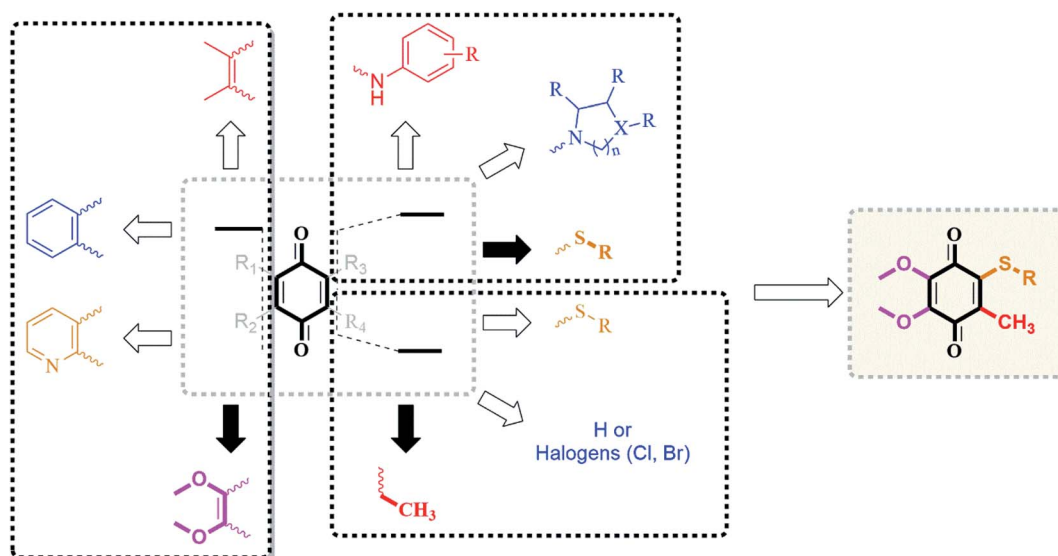

Fig. 2 Design strategy by the incorporation of **CoQ0** and alkyl chain thiols as the substrates based on our previous results in the literature.

obtained strains of Methicillin resistant *Staphylococcus aureus*, and bactericidal time-kill kinetic study. The most active analogs against *S. aureus* were employed in a molecular docking study within thymidylate kinase TMK, a crucial factor for DNA biosynthesis[40,41] and DNA gyrase enzyme which is essential for transcription and replication process of DNA molecule.[42,43]

2. Results and discussion

2.1. Library design and synthesis

The reactions between 1,4-quinones and nucleophiles such as amines, thiols, and alcohols[44] addressing to the lead molecules have been extensively studied. Depending upon the substitution pattern of 1,4-quinones, in contrast to amines, generally, thiols and alcohols could generate the disubstituted products in addition to monosubstituted products. The thiolated vitamin K3 analogs containing alkyl chain thio groups were recently investigated by our group and proved to be potent, selective, and active for inhibition bacterial formation. Table 1 outlines the synthesis of the thiolated **CoQ0** analogs (**CoQ1–8**) from the reaction of **CoQ0** with a range of alkyl chain thiols in good to high yields. The commercially available **CoQ0** was directly thiolated by the corresponding alkyl chain thiols in ethanol in one step (Table 1) by adopting the procedure in the literature.[10,45] In connection with this, we have obtained only one product because of the presence of the methyl group instead of halogen or hydrogen atom within the 1,4-quinone moiety. All the reactions were monitored by thin-layer chromatography with the disappearance of the **CoQ0**, then purified *via* silica gel column chromatography.

The structures of the thiolated **CoQ0** analogs (**CoQ1–8**) were examined by ^{1}H and ^{13}C nuclear magnetic resonance (NMR), mass spectroscopy (MS), and Fourier-transform infrared spectroscopy (FTIR). High-resolution mass spectra (HRMS) was registered to confirm the characterization of the thiolated **CoQ0** analogs (**CoQ1–8**). Additionally, the crystal structure of methyl-2-(4,5-dimethoxy-2-methyl-3,6-dioxocyclohexa-1,4-dienylthio) acetate (**CoQ1**) was determined by single-crystal X-ray diffraction analysis (Fig. 3). Suitable crystals for X-ray diffraction were

obtained by slow evaporation of ethanol solutions of the analog (**CoQ1**). The ORTEP drawings of the **CoQ1** was reported at 50% probability level in Fig. 3. The crystal system of the **CoQ1** is monoclinic (space group $P12_1/n1$) with the unit cell parameters $a = 3.9584$, $b = 23.942$, $c = 13.7731$. The crystallographic and structure refinement data for the analog (**CoQ1**) are summarized (for details, please see the Tables S2–S6 in the ESI file†). The average values of C–S bond lengths of the analog (**CoQ1**) are approximately 1.78 Å. The O4–C12, O5–C9 and O1–C1 bond lengths (about 1.44 Å) between sp^3 hybridized oxygen and carbon atoms are longer than the O4–C10, O5–C8, O1–C2 bond lengths (about 1.34 Å) between sp^3 hybridized oxygen atoms and sp^2 hybridized carbon atoms. These bonds are characteristic singlet bonds. However, the bond lengths of C11–O3, C7–O6, and O2–C2 are about 1.21 Å, confirming them as characteristic double bonds. Torsion angle, especially O3–C11–C4–S1 (9.4°), shows sulfur and oxygen atoms are not the same plane but close to each other. This allows to be formed hydrogen bonds between oxygen atom of carbonyl group and methylene protons. Besides, the long range interactions between oxygen (O5) of methoxy group and the methyl protons (C1H1) of the ester group as a hydrogen bond over the quinone ring shows in the Tables S2–S6 in the ESI† file.

2.2. Biological activity

2.2.1. Determination of minimum inhibitory concentrations (MIC) and structure–activity relationships (SARs) study. We investigated *in vitro* antibacterial and antifungal profile of the obtained thiolated **CoQ0** analogs (**CoQ1–8**) in relation to four Gram-negative bacteria (*Pseudomonas aeruginosa* ATCC 27853, *Escherichia coli* ATCC 25922, *Klebsiella pneumoniae* ATCC 4352, and *Proteus mirabilis* ATCC 14153), three Gram-positive bacteria (*Staphylococcus aureus* ATCC 29213, *Staphylococcus epidermidis* ATCC 12228, and *Enterococcus faecalis* ATCC 29212), and three fungi (*Candida albicans* ATCC 10231, *Candida parapsilosis* ATCC 22019, and *Candida tropicalis* ATCC 750) using the commercially available reference drugs (ceftazidime, cefuroxime-Na, cefuroxime, amikacin, clotrimazole, and

Table 1 Construction of the thiolated **CoQ0** analogs (**CoQ1–8**)

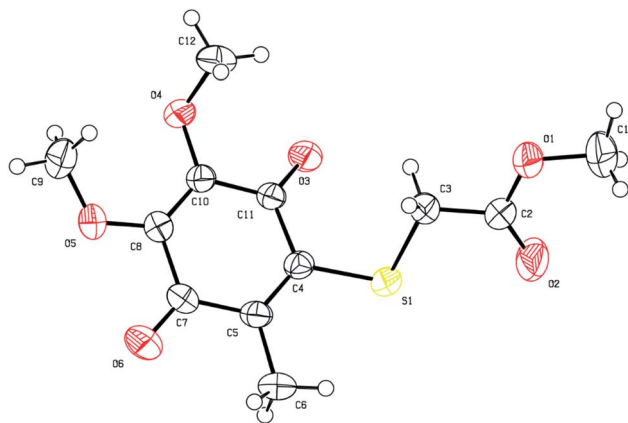| ID, yield (%)	R$_1$	R$_2$	ID, yield (%)	R$_1$	R$_2$
CoQ1 ($n = 1$), 75	H	CH$_3$	**CoQ5** ($n = 2$), 39	H	CH$_2$CH$_3$
CoQ2 ($n = 1$), 52	H	CH$_2$CH$_3$	**CoQ6** ($n = 2$), 23	H	(CH$_2$)$_3$CH$_3$
CoQ3 ($n = 1$), 62	CH$_3$	CH$_2$CH$_3$	**CoQ7** ($n = 1$), 79	H	CH$_2$CH(n-C$_2$H$_5$)(CH$_2$)$_3$CH$_3$
CoQ4 ($n = 2$), 36	H	CH$_3$	**CoQ8** ($n = 2$), 65	H	(CH$_2$)$_5$CH(CH$_3$)$_2$

RSC Advances

Fig. 3 ORTEP drawings of **CoQ1** (2150434) at 50% probability level.

amphotericin B). We used the broth microdilution technique for microbiological tests to determine a minimum inhibitory concentration (MIC) values, listed in Tables 2 and 3 using the Clinical Laboratory Standards Institute (CLSI) recommendations.[46,47]

Some analogs (**CoQ3** and **CoQ5–8**) having alkyl chain thio groups were totally inactive against all Gram-negative bacterial strains. Surprisingly, **CoQ1**, **CoQ2**, and **CoQ4** showed weak antibacterial potency against all Gram-negative bacterial strains. On the other hand, to our delight, it can be seen from the data in Table 2 that the thiolated CoQ analog (**CoQ1**) was the most potent active against *S. aureus* and *S. epidermidis* among all obtained analogs, while **CoQ2** and **CoQ5** were the most active analogs against *E. faecalis* having MIC value 39.06 μg mL^{-1}. It is noteworthy to mention that three thiolated CoQ (**CoQ2**, **CoQ4**, and **CoQ5**) were the other attractive analogs on *S. aureus* with MIC value of 9.76 μg mL^{-1}. These analogs were found to be the stronger antibacterial lead molecules against some Gram-positive bacterial strains as compared to reference drugs. Excitingly, when we examined the antibacterial profile of the thiolated CoQ analogs against *S. epidermidis* strains, apart from **CoQ1**, we observed that two other analogs (**CoQ2** and **CoQ4**) had the same potent activity with the reference drug Cefuroxime, MIC = 9.76 μg mL^{-1}. Of all examined for antibacterial activity against *E. faecalis* strains, **CoQ1–5** displayed the remarkable activity (MIC range = 39.06–156.25 μg mL^{-1}). In particular, **CoQ2** and **CoQ5** showed the highest activity as the most potent analogs against *E. faecalis*, whereas **CoQ1** and **CoQ3** had 1.6-fold more potent analogs when compared reference standard Amikacin (MIC = 78.12 μg mL^{-1}). Notably, **CoQ4** exhibited good antibacterial activity against *E. faecalis* with MIC value (156.25 μg mL^{-1}).
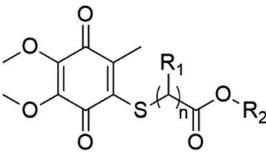
Concerning the three fungal strains, less activity was observed against *C. albicans*, *C. parapsilosis*, and *C. tropicalis*, and these molecules displayed antifungal activity with MIC values ranging between 78.12 and 1250 μg mL^{-1}. However these moderate activity could be achieved by penetrating into the fungal cell *via* the cellular membrane by passive diffusion with the greater lipophilic characters of these molecules.[48] Among the tested thiolated CoQ analogs, two CoQ analogs (**CoQ1** and

Table 2 The minimum inhibitory concentration (MIC) value of the thiolated CoQ analogs (CoQ1–8) for antibacterial activity[a]

Thiolated CoQ		Substituents		Gram-negative bacteria (MIC, μg mL^{-1})				Gram-positive bacteria (MIC, μg mL^{-1})		
General formula	ID	R$_1$	R$_2$	*P. aeruginosa*	*E. coli*	*K. pneumoniae*	*P. mirabilis*	*S. aureus*	*S. epidermidis*	*E. faecalis*
	CoQ1 (n = 1)	H	–CH$_3$	625	625	1250	1250	2.44	4.88	78.12
	CoQ2 (n = 1)	H	–CH$_2$CH$_3$	1250	1250	1250	1250	9.76	9.76	39.06
	CoQ3 (n = 1)	CH$_3$	–CH$_2$CH$_3$	—	—	—	—	19.53	—	78.12
	CoQ4 (n = 2)	H	–CH$_3$	1250	1250	—	1250	9.76	9.76	156.25
	CoQ5 (n = 2)	H	–CH$_2$CH$_3$	—	—	—	—	9.76	—	39.06
	CoQ6 (n = 2)	H	–(CH$_2$)$_3$CH$_3$	—	—	—	—	156.25	—	312.50
	CoQ7 (n = 1)	H	–CH$_2$CH(n-C$_2$H$_5$)(CH$_2$)$_3$CH$_3$	—	—	—	—	156.25	—	—
	CoQ8 (n = 2)	H	–(CH$_2$)$_5$CH(CH$_3$)$_2$	—	—	—	—	1250	—	—
	Ceftazidime			2.44	4.88	4.88	2.44	1.22		
	Cefuroxime-Na									
	Cefuroxime								9.76	
	Amikacin									128.00

[a] "—" means no activity.

Table 3 The minimum inhibitory concentration (MIC) value of the thiolated CoQ analogs (**CoQ1–8**) for antifungal activity[a]

| Thiolated CoQ		Substituents		Fungi (MIC, µg mL^{-1})		
General formula	ID	R$_1$	R$_2$	C. albicans	C. parapsilosis	C. tropicalis
	CoQ1 ($n = 1$)	H	–CH$_3$	625	156.25	312.50
	CoQ2 ($n = 1$)	H	–CH$_2$CH$_3$	1250	312.50	312.50
	CoQ3 ($n = 1$)	CH$_3$	–CH$_2$CH$_3$	—	78.12	—
	CoQ4 ($n = 2$)	H	–CH$_3$	1250	312.50	312.50
	CoQ5 ($n = 2$)	H	–CH$_2$CH$_3$	—	78.12	312.50
	CoQ6 ($n = 2$)	H	–(CH$_2$)$_3$CH$_3$	—	78.12	—
	CoQ7 ($n = 1$)	H	–CH$_2$CH(n-C$_2$H$_5$)(CH$_2$)$_3$CH$_3$	—	156.25	—
	CoQ8 ($n = 2$)	H	–(CH$_2$)$_5$CH(CH$_3$)$_2$	—	—	—
			Clotrimazole	4.9		
			Amphotericin B		0.5	1

[a] "—" means no activity.

CoQ2) showed strong antibacterial potency. The most promising thiolated CoQ analogs, **CoQ1** and **CoQ2**, with the highest antibacterial efficacy on Gram-positive bacterial strains, were chosen for further evaluation in order to establish their mode of action. Thus, we mainly focused on these two CoQ analogs for antimicrobial potency against clinically obtained Methicillin-resistant strains of *Staphylococcus aureus*. The *in vitro* activities of the **CoQ1** and **CoQ2** against 20 clinically isolates of MRSA are summarized in Fig. 4. The *in vitro* activity of selected molecules (**CoQ1** and **CoQ2**) had strong antimicrobial efficiency with the MIC$_{50}$ value 19.53 µg mL^{-1} on the studied strains. With this promising activity results, we focused further analysis of these potent antimicrobial effective molecules as drug candidate molecules.

In order to understand the effect of alkyl chain moiety of the thiol on the biological profile of the thiolated CoQ analogs, we analyzed the structural features with their MIC values of the CoQ analogs by manipulating the backbone group attached to the oxygen atom while keeping the methylene bridge(s) or methine bridge between the sulfur and carbonyl group of the substrates. Apparently, there is a simple correlation between the alkyl chain of the thiol and biological activity. The

presented data clearly showed that either the elongation of the methylene bridge or the insertion of the long-chain alkyl group attached to the oxygen atom starting from methyl, ethyl, and butyl group into the alkyl chain thiol decreased the biological potency, in particular against *S. aureus* and *S. epidermidis*. The efficacy against *S. aureus* and *S. epidermidis* decreased with the insertion of additional methyl group instead of hydrogen atom in methylene bridge in the thiolated CoQ analogs (**CoQ3**). In general, we could understand that a manipulation of the methylene bridge (elongation of the methylene bridge or insertion of methyl group) decreases the activity. Besides, changing the methyl to ethyl or butyl group decreased the potency by the elongation of the alkyl chain attached to the oxygen atom.

2.2.2. Time-kill kinetic study. Two most active compounds **CoQ1** and **CoQ2** were selected from the library after analyzing *in vitro* antimicrobial activity for further investigation of the mode of the action. Time-kill studies for **CoQ1** and **CoQ2** were performed on one clinically obtained Methicillin resistant *Staphylococcus aureus* isolate and the results are given in Fig. 5.

The results of the TKC studies did not show bactericidal activity (with a 3log$_{10}$ kill determined) for the studied strain at
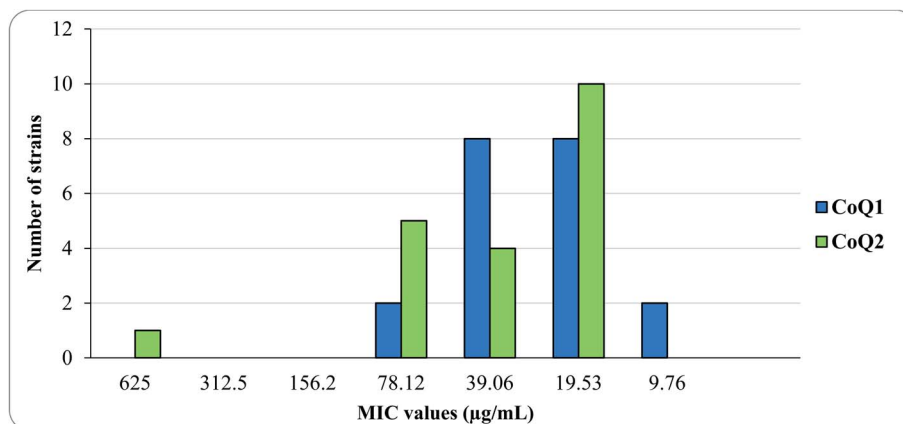
Fig. 4 The MIC distribution of **CoQ1** and **CoQ2** against 20 clinically obtained Meticillin-Resistant *Staphylococcus aureus* isolates.

$1\times$ and $4\times$ MIC concentrations within 24 h (Fig. 5). Even if the tested molecules decreased the viable cell count at 6 h for the tested strain, within the 24 h, bacterial regrowth was seen when the tested molecules used alone. In the era of antimicrobial resistance, it may be reasonable to examine the effects of these molecules which have low MIC values but results bacterial regrowth at 24 h when used alone, to show synergistic activity in combination with antibiotics frequently used in clinics.

2.2.3. Evaluation of the *in vitro* antibiofilm activity. Biofilms are described as a cluster multicellular surface-attached communities of bacteria embedded in self-produced extracellular matrix and they are commonly attached to living or nonliving surfaces and may be widespread in nature, hospital settings, and industry.[49,50] The biofilm lifestyle allows the bacteria to withstand hostile environmental conditions like starvation, desiccation and makes them capable to cause a broad range of chronic diseases. Hence, it is considered as a major cause of persistent nosocomial infections. Around 50% of the nosocomial infections are known biofilm-related.[51]

Biofilm development process has 4 stages: (1) attachment of bacterial cells to a suitable biotic/abiotic surface, (2) development of biofilm structure, (3) maturation of biofilm, and (4) dispersion. The investigation of the efficient antibiofilm molecules is targets of these stages especially the first two stages which are highly important for the biofilm development.[50,52] For this reason, we purposed to determine the antibiofilm effects of **CoQ1** and **CoQ2** against the first two stages of clinically obtained MRSA biofilms. When the $1/10\times$ MICs of tested molecules were examined for 1, 2, or 4 hours at 37 °C for MRSA's adherence to the wells of tissue culture microtiter plates, the tested agents inhibited biofilm attachment processes at least 50% for **CoQ2** at 4 h. In general, the inhibition rates of adhesion showed a time-dependent effect for MRSA (Fig. 6). When we evaluated the % biofilm formation of the studied strains, the rates of biofilm formation inhibition were dependent on

concentration; the highest inhibition rates were shown at $1\times$ MICs for the tested molecule, except for **CoQ2** (Fig. 6). For **CoQ2** molecule, $1\times$ MIC and $1/10\times$ MIC concentrations showed the same moderate activity against the tested MRSA's biofilms formation.

2.2.4. Molecular docking study. In the field of drug discovery and design, molecular docking calculations have become one of the most important tools to explore ligand/protein interactions. In a trial to elucidate their mechanism of action, we performed a docking study of our lead compounds with *S. aureus* TMK[41] and DNA gyrase.[53] The latter is classified as topoisomerase II enzyme that play crucial role in the transcription and replication process of DNA molecule. It has a pivotal role in all types of bacteria except higher eukaryotes. This makes DNA gyrase an attractive target for designing new antimicrobial drugs.[43,54] The interactions of **CoQ1** and **CoQ2** with TMK revealed a weak affinity, hence it is unlikely for TMK to be their molecular target (data not shown). However, their interactions with DNA gyrase showed interesting results that are in accordance with the *in vitro* output. **CoQ1** demonstrated strong molecular interactions with key amino acid residues. Its side chain has been implicated in two strong H-bonds with Arg144 and its quinone has two H–Pi bonds with Ile86. The main difference from the co-crystallized native ligand is only missing an interaction with Asp48. However, **CoQ2** quinone scaffold has formed one H-bond with Thr173 and one H–Pi bond with Ile86. The terminal hydrophobic alkyl side chain extends between unfavorable polar Arg144 and Arg84 residues, that is why longer alkyl chain abolishes the activity (Fig. 7).

2.2.5. *In silico* drug-likeness and ADME analysis of CoQ1 and CoQ2. Drug-likeness and ADME prediction of new chemical entities is significant in modern medicinal chemistry. SwissADME server, a free tool for drug likeness prediction, was applied for calculating several molecular and structural features of **CoQ1** and **CoQ2**. Both compounds can be easily transported
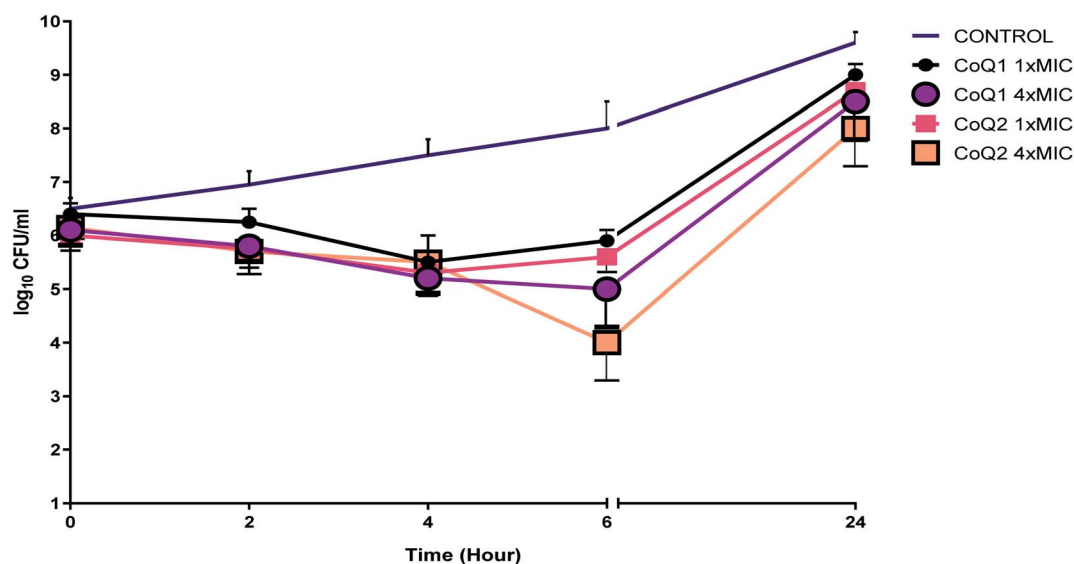

Fig. 5 Time-kill determinations for clinically resistant MRSA isolate after treatment with **CoQ1** and **CoQ2** at $1\times$ and $4\times$ MIC, respectively. The x-axis represents the killing time, and the y-axis represents the logarithmic MRSA survival.
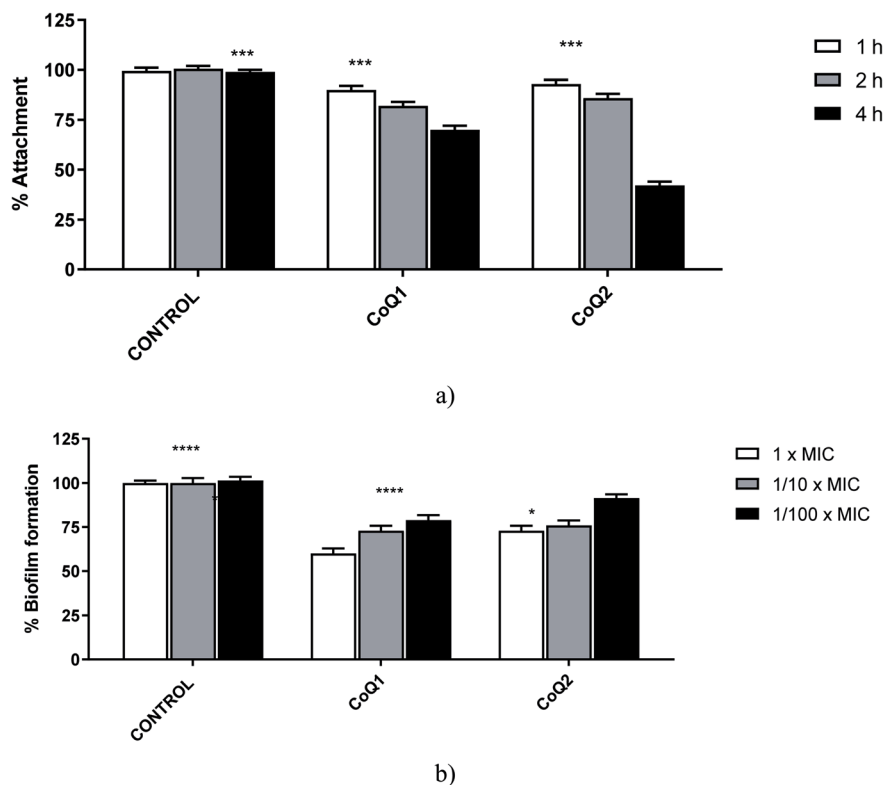
Fig. 6 Inhibition of MRSA. (a) Surface attachment to the wells contained 1/10× MIC of molecules and an inoculum of 1×10^6 CFU/200 μL, incubated for 1, 2, or 4 h at 37 °C for MRSA. (b) Biofilm formation in each well contained 1×, 1/10×, or 1/100× MIC of molecules and an inoculum of 1×10^6 to 1×10^7 CFU/200 μL, incubated for 24 h at 37 °C for MRSA. Control bars indicate microorganisms without molecules accepted as 100%. Six wells were used for the tested molecule. Each experiment is representative of two independent tests. All differences between the control and molecules treated biofilms were statistically significant (****$p < 0.005$).

in the body due to their small molecular weight (286 g mol^{-1} for **CoQ1** and 300 g mol^{-1} for **CoQ2**). This small molecular weight makes them ideal lead compounds that can be modified to enhance their affinity towards their target. Their octanol–water partition coefficient (log P), which indicates lipophilicity, is in the acceptable range (−0.4–5.6) Table 4. They have the same total polar surface area TPSA 104.20 Å^2 indicating potential

good bioavailability. Furthermore, the number of hydrogen bond acceptors (HBA < 10) and number of hydrogen bond donors (HBD < 5), are in the acceptable ranges. SwissADME calculations revealed that the titled compounds possess lead-likeness properties[55] and they obey all of Lipinski,[56] Ghose,[57] Veber,[58] Egan,[59] and Muegge[60] rules for drug-likeness without any violations (Table 5).
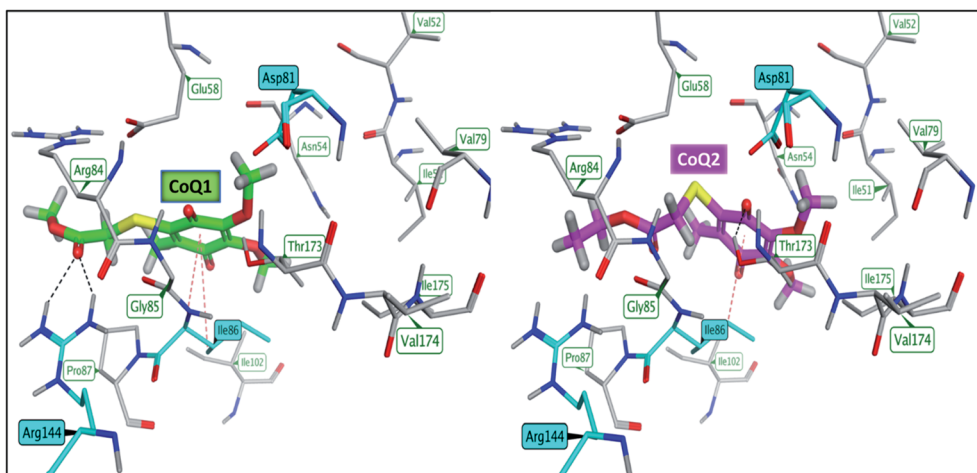

Fig. 7 Binding mode of **CoQ1** (left) and **CoQ2** (right) into the ligand binding site of *S. aureus* DNA gyrase (PDB: 3G75).

Table 4 Physico-chemical properties and drug-likeness prediction

Property/rule	CoQ1	CoQ2
MW	286	300
Log P	2.17	2.24
TPSA (Å^2)	104.20	104.20
HBA	6	6
HBD	0	0
Lipiniski	Yes, 0 violation	Yes, 0 violation
Ghose	Yes	Yes
Veber	Yes	Yes
Egan	Yes	Yes
Muegge	Yes	Yes
Leadlikeness	Yes	Yes

Table 5 ADME prediction

Property	CoQ1	CoQ2
BBB permeability	No	No
GI absorption	High	High
Log S	−2.11	−2.36
Solubility	Soluble	Soluble
Bioavailability score	0.56	0.56
CYP1A2, CYP2C9, CYP2D6, CYP3A4	No	No

ADME properties of **CoQ1** and **CoQ2** showed promising profiles as well. In SwissADME, they use a BOILED-Egg model that showed that both compounds can't pass through blood–brain barrier (BBB) which help avoid side effects on central nervous system (CNS). They also likely to have a good gastrointestinal (GI) absorption which is attributed to their ability to passively absorbed by the GIT. They have a quite good solubility[61] and bioavailability score.[62] Furthermore, they have no interference with metabolic enzymes cytochrome P450 isoforms CYP1A2, CYP2C9, CYP2D6, and CYP3A4.

3.   Conclusions

We have successfully demonstrated that the thiolated CoQ analogs show promising structures as a template for the development of antibiotics on a sustainable basis due to the fact that further efforts for optimization are required before these thiolated CoQ analogs can be turned into valuable lead molecules for bacterial infections. In conclusion, we designed and synthesized a series of the thiolated CoQ analogs (**CoQ1–8**) for their antimicrobial activity. In addition to design and synthesis, we tested *in vitro* antimicrobial activity assays on seven different bacterial strains and three different fungal strains by using serial dilution method. The obtained results indicated that the antibacterial activity of the CoQ analogs increased by the insertion of alkyl chain thiols into the CoQ core. Extensive antibacterial tests for the most promising molecules (**CoQ1** and **CoQ2**) on bacterial strains, *S. aureus*, *S. epidermidis*, and *E. faecalis* resulted in new potential analogs against bacterial infections. Furthermore, two thiolated CoQ analogs (**CoQ1** and **CoQ2**) were also used for understanding the mode of action by

evaluating the time-kill kinetic study. Also, we carried out another study on two analogs, active on *S. aureus*, *via* determining its biofilm inhibition capacities. **CoQ1** and **CoQ2** demonstrated strong molecular interactions with DNA gyrase with optimal lead like pharmacokinetic profile. **CoQ1** and **CoQ2** demonstrated strong molecular interactions with DNA gyrase with optimal lead like pharmacokinetic profile.

As far as we know, our study is the first record to evaluate the antibiofilm and bactericidal activities of the thiolated CoQ analogs against clinically resistant species. In line with this view, in our study, **CoQ1** and **CoQ2** showed potent antimicrobial activity against the clinically obtained MRSA strains with the 19.53 μg mL^{-1} MIC$_{50}$. Although, in accordance with the time-kill curve studies results, these molecules showed bacterial regrowth at 1× and 4× MIC concentration used within 24 h against Methicillin-resistant *S. aureus* isolate, these molecules achieved decreased viable cell count at 6 h. So, to achieve synergistic activity, it would be possible to use these molecules in combination with conventional antibiotics, to reduce the antibiotic toxicity and reducing to antimicrobial resistance. Moreover, the results obtained from antibiofilm activity studies reveal that these molecules can be considered for future studies on dispersal of MRSA biofilms. In conclusion, the potential antibacterial activity of the thiolated CoQ analogs (**CoQ1–8**) afford them a potential to be developed as novel antibacterial drugs.

4.   Experimental

4.1.   Chemicals and apparatus

Reagents and solvents were of analytical grade and were purchased from commercial suppliers with a minimum purity of 95%), and used as received. Melting points (mp) were determined on electrical melting point (Büchi B-540) and are uncorrected. The Fourier transform infrared spectra were recorded on a Alpha T FTIR spectrometer equipped with single reflection diamond ATR module. ^{1}H NMR and ^{13}C NMR spectra were acquired on a Bruker for the characterization of the purified analogs. The ^{1}H NMR spectra data is expressed in the form: chemical shifts in units of parts per million (ppm) in CDCl$_3$ and coupling constants (J) are in hertz (Hz). Mass spectra were recorded on a BRUKER Microflex LT by MALDI (Matrix Assisted Laser Desorption Ionization)-TOF technique *via* addition of 1,8,9-anthracenetriol (DIT, dithranol) as matrix. High-resolution mass spectra electrospray ionization (HRMS-ESI) were obtained on a Waters SYNAPT G1 MS by dissolving analogs (2–3 mg) in acetonitrile. Thin layer chromatography (TLC) was performed with silica gel coated aluminum sheets from Merck KGaA. TLC visualization was carried out by using UV light (254 nm). All synthesized thiolated CoQ analogs were purified by column chromatography with a silica gel 60 (63–200 μm particle sized) with appropriate solvent system as eluent.

4.2.   X-ray diffraction analysis

Data for the single crystal compounds were obtained with Bruker APEX II QUAZAR three-circle diffractometer. Indexing

was performed using APEX2.[63] Data integration and reduction were carried out with SAINT.[64] Absorption corrections were performed by multi-scan method implemented in SADABS.[65] The Bruker SHELXTL[66] software package was used for structures solution and structures refinement. Crystal structure validations and geometrical calculations were performed using the Platon software.[67] Mercury software[68] was used for visualization of the .cif files. The crystallographic and structure refinement data, the selected bond lengths, bond angles, torsion angles, hydrogen bond distances, and angles are given in the Tables S2–S6 in the ESI file†). The crystallographic data have been deposited at the Cambridge Crystallographic Data Centre, and CCDC reference numbers is 2150434 for **CoQ1**.†

4.3. General procedure for the synthesis of coenzyme Q (CoQ) analogs

To a stirred solution of **CoQ** (100 mg, 1 eq.) in ethanol (20 mL) was added corresponding thiol (1 eq.) dropwise at room temperature. The reaction mixture was then refluxed until consumption of starting material. The reaction mixture was cooled to ambient temperature. After the reaction mixture was concentrated under reduced pressure, the residue was dissolved with CH_2Cl_2 (50 mL), and the solution was washed sequentially with water (3 × 30 mL). The organic layer was dried over $CaCl_2$, filtered, and concentrated under reduced pressure, and the residue was purified by means of column chromatography on silica gel to afford desired products (**CoQ** analogs).

4.3.1. Methyl-2-(4,5-dimethoxy-2-methyl-3,6-dioxocyclohexa-1,4-dienylthio)acetate (CoQ1).

The general procedure was followed using methyl thioglycolate (60 mg, 1 eq.) and CoQ. Purification by column chromatography on silica gel (PET/EtAc, v/v 5 : 1) yielded **CoQ1** (75%) as a yellow viscose oil. FTIR (ATR) v (cm^{-1}): 2947, 2856 ($CH_{aliphatic}$), 1738, 1661, 1631 (>C=O), 1582, 1436, 1376, 1302, 1257, 1194, 1172, 1128, 1104; ^1H NMR (500 MHz, $CDCl_3$) δ (ppm): 3.99 (s, 3H, OCH_3), 3.95 (s, 3H, OCH_3), 3.83 (s, 2H, SCH_2), 3.69 (s, 3H, OCH_3), 2.17 (s, 3H, CH_3); ^{13}C NMR (125 MHz, $CDCl_3$) δ (ppm): 181.6, 180.1, 169.6 (>C=O), 145.0, 144.8, 143.1, 139.7 (C_q), 61.3, 61.1, 52.6 (OCH_3), 34.7 (SCH_2), 14.3 (CH_3); Anal. calcd for $C_{12}H_{14}O_6S$: C, 50.34; H, 4.93; found: C, 49.92; H, 5.02; MS (MALDI TOF) m/z: 288 [M + 2H]$^+$, Anal. calcd for $C_{12}H_{14}O_6S$ (286.05); HRMS (TOF MS ES+) m/z calcd for $C_{12}H_{15}O_6S$ [M + H]$^+$: 287.0589; found: 287.0591; calcd for $C_{12}H_{14}O_6SNa$ [M + Na]$^+$: 309.0409; found: 309.0414.

4.3.2. Ethyl-2-(4,5-dimethoxy-2-methyl-3,6-dioxocyclohexa-1,4-dienylthio)acetate (CoQ2).

The general procedure was followed using ethyl thioglycolate (66 mg, 1 eq.) and CoQ. Purification by column chromatography on silica gel (PET/EtAc, v/v 5 : 1) yielded **CoQ2** (52%) as a yellow viscose oil. FTIR (ATR) v (cm^{-1}): 2993, 2959, 2936, 2856 ($CH_{aliphatic}$), 1742, 1664, 1649, 1628 (>C=O), 1582, 1296, 1259, 1175, 1129, 1106, 1025, 1003; ^1H NMR (500 MHz, $CDCl_3$) δ (ppm): 4.15 (q, J = 7.1 Hz, 2H, OCH_2), 4.01 (s, 3H, OCH_3), 3.97 (s, 3H, OCH_3), 3.83 (s, 2H, SCH_2), 2.19 (s, 3H, CH_3), 1.24 (t, J = 7.1 Hz, 3H, OCH_2CH_3); ^{13}C NMR (125 MHz, $CDCl_3$) δ (ppm): 181.6, 180.1, 169.1 (>C=O), 145.0, 144.8, 143.1, 139.9 (C_q), 61.6 (OCH_2), 61.3, 61.2 (OCH_3),

34.9 (SCH_2), 14.3, 14.1 (CH_3); Anal. calcd for $C_{13}H_{16}O_6S$: C, 51.99; H, 5.37; found: C, 51.85; H, 5.12; HRMS (TOF MS ES+) m/z calcd for $C_{13}H_{17}O_6S$ [M + H]$^+$: 301.0746; found: 301.0746; calcd for $C_{13}H_{16}O_6SNa$ [M + Na]$^+$: 323.0565; found: 323.0575.

4.3.3. Ethyl-2-(4,5-dimethoxy-2-methyl-3,6-dioxocyclohexa-1,4-dienylthio)propanoate (CoQ3).

The general procedure was followed using ethyl-2-mercaptopropanoate (73 mg, 1 eq.) and CoQ. Purification by column chromatography on silica gel (PET/EtAc, v/v 5 : 1) yielded **CoQ3** (62%) as a yellow viscose oil. FTIR (ATR) v (cm^{-1}): 2983, 2944, 2848 ($CH_{aliphatic}$), 1733, 1657, 1634 (>C=O), 1584, 1451, 1376, 1300, 1247, 1198, 1130, 1093; ^1H NMR (500 MHz, $CDCl_3$) δ (ppm): 4.35 (q, J = 7.1 Hz, 1H, SCHCH_3), 4.25–4.06 (m, 2H, OCH_2), 4.02 (s, 3H, OCH_3), 4.00 (s, 3H, OCH_3), 2.19 (s, 3H, CH_3), 1.52 (d, J = 7.1 Hz, 3H, CHCH_3), 1.21 (t, J = 7.1 Hz, 3H, OCH_2CH_3); ^{13}C NMR (125 MHz, $CDCl_3$) δ (ppm): 182.0, 180.0, 171.8 (>C=O), 145.2, 144.9, 144.4, 140.3 (C_q), 61.4 (OCH_2), 61.3, 61.1 (OCH_3), 43.3 (SCH), 16.7, 14.6, 14.1 (CH_3); Anal. calcd for $C_{14}H_{18}O_6S$: C, 53.49; H, 5.77; found: C, 53.22; H, 5.56; HRMS (TOF MS ES+) m/z calcd for $C_{14}H_{19}O_6S$ [M + H]$^+$: 315.0902; found: 315.0901.

4.3.4. Methyl-3-(4,5-dimethoxy-2-methyl-3,6-dioxocyclohexa-1,4-dienylthio)propanoate (CoQ4).

The general procedure was followed using methyl 3-mercaptopropanoate (66 mg, 1 eq.) and CoQ. Purification by column chromatography on silica gel (PET/EtAc, v/v 5 : 1) yielded **CoQ4** (36%) as a yellow viscose oil. FTIR (ATR) v (cm^{-1}): 2962, 2919, 2848 ($CH_{aliphatic}$), 1738, 1659, 1631 (>C=O), 1579, 1430, 1354, 1302, 1242, 1187, 1128, 1097; ^1H NMR (500 MHz, $CDCl_3$) δ (ppm): 4.02 (s, 3H, OCH_3), 4.01 (s, 3H, OCH_3), 3.69 (s, 3H, OCH_3), 3.32 (t, J = 7.0 Hz, 2H, SCH_2), 2.68 (t, J = 7.0 Hz, 2H, CH_2(C=O)), 2.18 (s, 3H, CH_3); ^{13}C NMR (125 MHz, $CDCl_3$) δ (ppm): 181.8, 180.3, 171.9 (>C=O), 145.1, 144.8, 143.6, 140.8 (C_q), 61.4, 61.2, 51.9 (OCH_3), 35.5 (SCH_2), 29.2 (CH_2(C=O)), 14.6 (CH_3); Anal. calcd for $C_{13}H_{16}O_6S$: C, 51.99; H, 5.37; found: C, 51.73; H, 5.39; HRMS (TOF MS ES+) m/z calcd for $C_{13}H_{17}O_6S$ [M + H]$^+$: 301.0746; found: 301.0745.

4.3.5. Ethyl-3-(4,5-dimethoxy-2-methyl-3,6-dioxocyclohexa-1,4-dienylthio)propanoate (CoQ5).

The general procedure was followed using ethyl 3-mercaptopropanoate (74 mg, 1 eq.) and **CoQ**. Purification by column chromatography on silica gel (PET/EtAc, v/v 5 : 1) yielded **CoQ5** (39%) as a yellow viscose oil. FTIR (ATR) v (cm^{-1}): 2985, 2947, 2848 ($CH_{aliphatic}$), 1730, 1655, 1634 (>C=O), 1580, 1452, 1370, 1298, 1247, 1191, 1131, 1097; ^1H NMR (500 MHz, $CDCl_3$) δ (ppm): 4.06 (q, J = 7.1 Hz, 2H, OCH_2), 3.94 (s, 3H, OCH_3), 3.93 (s, 3H, OCH_3), 3.23 (t, J = 7.0 Hz, 2H, SCH_2), 2.57 (t, J = 7.0 Hz, 2H, CH_2(C=O)), 2.10 (s, 3H, CH_3), 1.18 (t, J = 7.1 Hz, 3H, OCH_2CH_3); ^{13}C NMR (125 MHz, $CDCl_3$) δ (ppm): 181.8, 180.2, 171.4 (>C=O), 145.1, 144.8, 143.5, 140.9 (C_q), 61.3 (OCH_2), 61.2, 60.8 (OCH_3), 35.7 (SCH_2), 29.2 (SCH_2(C=O)), 14.6, 14.2 (CH_3); Anal. calcd. for $C_{14}H_{18}O_6S$: C, 53.49; H, 5.77; found: C, 53.77; H, 5.89; HRMS (TOF MS ES+) m/z calcd for $C_{14}H_{19}O_6S$ [M + H]$^+$: 315.0902; found: 315.0904.

4.3.6. Butyl-3-(4,5-dimethoxy-2-methyl-3,6-dioxocyclohexa-1,4-dienylthio)propanoate (CoQ6).

The general procedure was followed using butyl 3-mercaptopropanoate (89 mg, 1 eq.) and CoQ. Purification by column chromatography on silica gel (PET/EtAc, v/v 5 : 1) yielded **CoQ6** (23%) as a yellow viscose oil. FTIR (ATR) v (cm^{-1}): 2958, 2937, 2874 ($CH_{aliphatic}$), 1732, 1697, 1657

(>C=O), 1583, 1455, 1298, 1248, 1197, 1134, 1101, 1066; ^{1}H NMR (500 MHz, CDCl$_3$) δ (ppm): 4.01 (t, J = 6.7 Hz, 2H, OCH$_2$), 3.94 (s, 3H, OCH$_3$), 3.93 (s, 3H, OCH$_3$), 3.23 (t, J = 6.9 Hz, 2H, SCH$_2$), 2.58 (t, J = 6.9 Hz, 2H, CH$_2$(C=O)), 2.10 (s, 3H, CH$_3$), 1.57–1.47 (m, 2H, CH$_2$), 1.36–1.22 (m, 2H, CH$_2$), 0.86 (t, J = 7.4 Hz, 3H, CH$_3$); ^{13}C NMR (125 MHz, CDCl$_3$) δ (ppm): 181.8, 180.2, 171.5 (>C=O), 145.1, 144.8, 143.5, 140.9 (C$_q$), 64.7 (OCH$_2$), 61.3, 61.2 (OCH$_3$), 35.7 (SCH$_2$), 30.6 (SCH$_2$(C=O)), 29.2, 19.1 (CH$_2$), 14.5, 13.7 (CH$_3$); Anal. calcd for C$_{16}$H$_{22}$O$_6$S: C, 56.12; H, 6.48; found: C, 55.76; H, 6.33; HRMS (TOF MS ES+) m/z calcd for C$_{16}$H$_{23}$O$_6$S [M + H]$^+$: 343.1215; found: 343.1215.

4.3.7. 2-Ethylhexyl-2-(4,5-dimethoxy-2-methyl-3,6-dioxocyclohexa-1,4-dienylthio)acetate (CoQ7). The general procedure was followed using 2-ethylhexyl thioglycolate (112 mg, 1 eq.) and CoQ. Purification by column chromatography on silica gel (PET/EtAc, v/v 5 : 1) yielded **CoQ7** (79%) as a yellow viscose oil. FTIR (ATR) v (cm^{-1}): 2931, 2860 (CH$_{aliphatic}$), 1733, 1658, 1634 (>C=O), 1582, 1457, 1374, 1294, 1249, 1198, 1132, 1099; ^{1}H NMR (500 MHz, CDCl$_3$) δ (ppm): 4.10–3.93 (m, 8H, OCH$_2$ + OCH$_3$), 3.87 (s, 2H, SCH$_2$), 2.19 (s, 3H, CH$_3$), 1.63–1.46 (m, 1H, CH), 1.41–1.13 (m, 8H, CH$_2$), 0.96–0.82 (m, 6H, CH$_3$); ^{13}C NMR (125 MHz, CDCl$_3$) δ (ppm): 181.6, 180.1, 169.4 (>C=O), 145.0, 144.8, 142.9, 139.9 (C$_q$), 68.0 (OCH$_2$), 61.3, 61.1 (OCH$_3$), 38.7 (SCH$_2$), 34.9 (CH), 30.2, 28.9, 23.6, 22.9 (CH$_2$), 14.3, 14.0, 10.9 (CH$_3$); Anal. calcd for C$_{19}$H$_{28}$O$_6$S: C, 59.35; H, 7.34; found: C, 59.65; H, 7.39; HRMS (TOF MS ES+) m/z calcd for C$_{19}$H$_{29}$O$_6$S [M + H]$^+$: 385.1685; found: 385.1685.

4.3.8. 6-Methylheptyl-3-(4,5-dimethoxy-2-methyl-3,6-dioxocyclohexa-1,4-dienylthio)propanoate (CoQ8). The general procedure was followed using isooctyl-3-mercaptopropionate (120 mg, 1 eq.) and CoQ. Purification by column chromatography on silica gel (PET/EtAc, v/v 5 : 1) yielded **CoQ8** (65%) as a yellow viscose oil. FTIR (ATR) v (cm^{-1}): 2956, 2926, 2874 (CH$_{aliphatic}$), 1733, 1658, 1634 (>C=O), 1579, 1455, 1365, 1296, 1248, 1197, 1132, 1097; ^{1}H NMR (500 MHz, CDCl$_3$) δ (ppm): 4.12–4.08 (m, 2H, OCH$_2$), 4.07–3.92 (m, 6H, OCH$_3$), 3.34–3.30 (m, 2H, SCH$_2$), 2.8–2.64 (m, 2H, SCH$_2$CH$_2$), 2.17 (s, 3H, CH$_3$), 1.78–1.48 (m, 4H, CH$_2$), 1.45–1.20 (m, 4H, CH$_2$), 1.20–1.10 (m, 1H, CH), 0.95–0.80 (m, 6H, CH$_3$); ^{13}C NMR (125 MHz, CDCl$_3$) δ (ppm): 181.7, 180.2, 171.5 (>C=O), 145.1, 144.8, 143.4, 140.9 (C$_q$), 63.4 (OCH$_2$), 61.3, 61.2 (OCH$_3$), 36.6 (SCH$_2$), 29.2 (SCH$_2$(C=O)), 27.4, 25.1, 23.3, 22.9, 22.2 (CH$_2$ and CH), 19.7, 14.6, 14.1 (CH$_3$); Anal. calcd for C$_{20}$H$_{30}$O$_6$S: C, 60.28; H, 7.59; found: C, 60.54; H, 7.29; MS (MALDI TOF) m/z: 398 [M–H]$^+$, Anal. calcd for C$_{20}$H$_{30}$O$_6$S (398.51); HRMS (TOF MS ES+) m/z calcd for C$_{20}$H$_{31}$O$_6$S [M + H]$^+$: 399.1841; found: 399.1840.

4.4. Biological evaluation

4.4.1. MIC evaluation. MICs of the molecules were examined by the broth microdilution technique approved by Clinical and Laboratory Institute (CLSI).[46,47] The inoculum of the tested four Gram negative (*Pseudomonas aeruginosa* ATCC 27853, *Escherichia coli* ATCC 25922, *Klebsiella pneumoniae* ATCC 4352, *Proteus mirabilis* ATCC 14153), three Gram positive (*Staphylococcus aureus* ATCC 29213, *Staphylococcus epidermidis* ATCC 12228, *Enterococcus faecalis* ATCC 29212), and three yeast

(*Candida albicans* ATCC 10231, *Candida parapsilosis* ATCC 22019, *Candida tropicalis* ATCC 750) were prepared by CLSI recommendations. The stock solutions of the tested molecules were prepared in DMSO. Serial two fold dilutions ranging from 1250 to 0.06 µg mL^{-1} were prepared in Mueller Hinton Broth for the tested bacteria and RPMI-1640 medium for the yeast, respectively.

According to the antimicrobial activity results, we aimed to identify *in vitro* activities of the **CoQ1** and **CoQ2** against clinically obtained strains by the broth microdilution dilution technique as described by the CLSI recommendations.[46,47] For this assay, 20 nonduplicate, nosocomially acquired Methicillin-resistant *Staphylococcus aureus* isolated from blood specimens between April and September 2017 were obtained from the Department of Infectious Diseases and Clinical Microbiology, Faculty of Medicine, Istanbul Medipol University. All strains were identified using API STAPH (bioM'erieux). Then, all the tested *S. aureus* isolates were chosen by using oxacillin susceptibility to determine the methicillin resistant isolates, approved by CLSI (MIC ≥ 4 µg mL^{-1}).[46] The MIC was defined as the lowest concentration of tested extracts giving complete inhibition of visible growth. Experiments were performed in triplicate.

4.4.2. Determination of time-kill curves. The bactericidal activity of selected molecules (**CoQ1** and **CoQ2**) was tested by the time-killing curve (TKC) method at one and four times the MIC against one (1) MRSA clinical strain. Molecules-free controls were included for the tested strain. Inocula were quantified spectrophotometrically and added to the flasks to yield a final concentration of 1×10^6 CFU mL^{-1}. The test tubes containing MHB with and without (growth control) molecules in a final volume of 10 mL were incubated in a 37 °C calibrated shaking water bath, and viable counts were determined at 0, 2, 4, 6, and 24 h intervals after inoculation, by subculturing 0.1 mL serial dilutions onto TSA plates. All tests were performed in duplicate. The lower limit of detection for time-kill assay was 1log$_{10}$ CFU per mL. Bactericidal activity was defined as a ≥3log$_{10}$ CFU per mL decrease from the initial inoculum.

4.4.3. Determination of the antibiofilm activities. Biofilm attachment and inhibition of biofilm formation assays were performed as previously described method with some modifications.[37] For biofilm attachment, an overnight culture of strong, biofilm-producing clinically MRSA isolate was diluted 1/50 to obtain 1×10^6 to 1×10^7 CFU/200 mL for bacteria in TSB supplement with 1% glucose. Then the strain was added to each well of 96-well tissue culture microtiter plates with 1/10× MIC of tested molecules. The plates were allowed to incubate for 1, 2, and 4 h at 37 °C. The positive control was studied strain in the using medium alone. After incubation, each well was washed with PBS solution three times and measured at OD 595 nm.

For inhibition of the biofilm formation, the tested strain was incubated in its medium and molecules at 1× and 1/10× in addition to 1/100× MIC in 37 °C for 24 h in microtiter plates. Six wells were used for each molecules. The positive control was the tested strain in its medium without molecules. After incubation, each well was washed with PBS solution three times and measured at OD 595 nm.

4.5. Statistical analysis

All experiments were performed in two independent assays. Two-way ANOVA-Tukey's multiple comparison test was used to compare differences between control and antimicrobials treated biofilms. P value <0.005 was considered as statistically significant.

4.6. Molecular docking

S. aureus DNA gyrase X-ray crystal structure (PDB code 3G75) [9] was retrieved from Protein Data Bank to be utilized as a model in the present study. The protein structure was prepared using QuickPrep module of MOE (version 2019.01, Chemical Computing Group Inc., Montreal, QCstate abbrev, Canada). Only one monomer, chain A, was selected and water residues were deleted. The docking study was conducted using the rigid-receptor method.[69,70] The co-crystallized ligand B48 was defined as the center of the binding site. Using the MOE build suite, the chemical structures were drawn, and then energy-minimized using the MOE default force field.[71] All other docking options were kept at their default values. Fifteen docking positions were generated for each ligand. The generated docking positions were visualized using MOE.

4.7. *In silico* drug-likeness and ADMET analysis

The online SwissADME server was employed to predict the drug-likeness and ADME parameters.[72]

Conflicts of interest

The authors declare no conflict of interest.

Acknowledgements

References

1 I. Abraham, R. Joshi, P. Pardasani and R. T. Pardasani, *J. Braz. Chem. Soc.*, 2011, **22**, 385–421.

2 C. E. Sansom, L. Larsen, N. B. Perry, M. V. Berridge, E. W. Chia, J. L. Harper and V. L. Webb, *J. Nat. Prod.*, 2007, **70**, 2042–2044.

3 S. Nojima, C. Schal, F. X. Webster, R. G. Santangelo and W. L. Roelofs, *Science*, 2005, **307**, 1104–1106.

4 D. Tasdemir, R. Brun, V. Yardley, S. G. Franzblau and P. Rüedi, *Chem. Biodiversity*, 2006, **3**, 1230–1237.

5 H. Bauer, K. Fritz-Wolf, A. Winzer, S. Kuhner, S. Little, V. Yardley, H. Vezin, B. Palfey, R. H. Schirmer and E. Davioud-Charvet, *J. Am. Chem. Soc.*, 2006, **128**, 10784–10794.

6 L. S. Lara, G. C. Lechuga, C. D. S. Moreira, T. B. Santos, V. F. Ferreira, D. R. da Rocha and M. C. S. Pereira, *Molecules*, 2021, **26**(2), 423.

7 M. Yamashita, J. Sawano, R. Umeda, A. Tatsumi, Y. Kumeda and A. Iida, *Chem. Pharm. Bull.*, 2021, **69**, 661–673.

8 N. Bayrak, H. I. Ciftci, M. Yildiz, H. Yildirim, B. Sever, H. Tateishi, M. Otsuka, M. Fujita and A. F. Tuyun, *Chem.-Biol. Interact.*, 2021, **345**, 109555.

9 A. T. Jannuzzi, M. Yıldız, N. Bayrak, H. Yıldırım, D. Shilkar, V. Jayaprakash and A. F. TuYuN, *Chem.-Biol. Interact.*, 2021, **349**, 109673.

10 H. Yildirim, N. Bayrak, M. Yildiz, E. M. Kara, B. O. Celik and A. F. Tuyun, *J. Mol. Struct.*, 2019, **1195**, 681–688.

11 C. Varricchio, K. Beirne, P. Aeschlimann, C. Heard, M. Rozanowska, M. Votruba and A. Brancale, *J. Med. Chem.*, 2020, **63**, 13638–13655.

12 K. W. Wellington, *RSC Adv.*, 2015, **5**, 20309–20338.

13 J. S. Novais, M. F. Carvalho, M. S. Ramundo, C. O. Beltrame, R. B. Geraldo, A. K. Jordao, V. F. Ferreira, H. C. Castro and A. M. S. Figueiredo, *Sci. Rep.*, 2020, **10**, 19631.

14 F. R. F. Dias, J. S. Novais, T. A. D. S. Devillart, W. A. da Silva, M. O. Ferreira, R. D. Loureiro, V. R. Campos, V. F. Ferreira, M. C. B. V. de Souza, H. C. Castro and A. C. Cunha, *Eur. J. Med. Chem.*, 2018, **156**, 1–12.

15 K. W. Wellington, N. B. P. Nyoka and L. J. McGaw, *Drug Dev. Res.*, 2019, **80**, 386–394.

16 P. Ravichandiran, M. Maslyk, S. Sheet, M. Janeczko, D. Premnath, A. R. Kim, B. H. Park, M. K. Han and D. J. Yoo, *Chemistryopen*, 2019, **8**, 589–600.

17 A. Alfadhli, A. Mack, L. Harper, S. Berk, C. Ritchie and E. Barklis, *Bioorg. Med. Chem.*, 2016, **24**, 5618–5625.

18 O. P. S. Patel, R. M. Beteck and L. J. Legoabe, *Eur. J. Med. Chem.*, 2021, **210**, 113084.

19 A. Kosiha, K. M. Lo, C. Parthiban and K. P. Elango, *Mater. Sci. Eng., C*, 2019, **94**, 778–787.

20 A. Kosiha, C. Parthiban and K. P. Elango, *J. Coord. Chem.*, 2018, **71**, 1560–1574.

21 P. Jayasudha, R. Manivannan, S. Ciattini, L. Chelazzi and K. P. Elango, *Sens. Actuators, B*, 2017, **242**, 736–745.

22 C. Parthiban and K. P. Elango, *Sens. Actuators, B*, 2017, **245**, 321–333.

23 J. Wang, F. Xia, W.-B. Jin, J.-Y. Guan and H. Zhao, *Bioorg. Chem.*, 2016, **68**, 214–218.

24 P. J. O'Brien, *Chem.-Biol. Interact.*, 1991, **80**, 1–41.

25 I. N. Okeke, K. P. Klugman, Z. A. Bhutta, A. G. Duse, P. Jenkins, T. F. O'Brien, A. Pablos-Mendez and R. Laxminarayan, *Lancet Infect. Dis.*, 2005, **5**, 568–580.

26 G. J. Basset, S. Latimer, A. Fatihi, E. Soubeyrand and A. Block, *Mini-Rev. Med. Chem.*, 2017, **17**, 1028–1038.

27 V. Weissig, *Trends Mol. Med.*, 2020, **26**, 40–57.

28 G. M. Enns, *J. Child Neurol.*, 2014, **29**, 1235–1240.

29 T. Meier and G. Buyse, *J. Neurol.*, 2009, **256**, 25–30.

30 E. M. Yubero-Serrano, L. Gonzalez-Guardia, O. Rangel-Zuñiga, N. Delgado-Casado, J. Delgado-Lista, P. Perez-Martinez, A. Garcia-Rios, J. Caballero, C. Marin, F. M. Gutierrez-Mariscal, F. J. Tinahones, J. M. Villalba, I. Tunez, F. Perez-Jimenez and J. Lopez-Miranda, *Age*, 2013, **35**, 159–170.

31 S. Pepe, S. F. Marasco, S. J. Haas, F. L. Sheeran, H. Krum and F. L. Rosenfeldt, *Mitochondrion*, 2007, **7**, S154–S167.

32 A. F. Tuyun, M. Yildiz, N. Bayrak, H. Yildirim, E. M. Kara, A. T. Jannuzzi and B. O. Celik, *Drug Dev. Res.*, 2019, **80**, 1098–1109.

33 N. Bayrak, H. Yildirim, A. F. Tuyun, E. M. Kara, B. O. Celik, G. K. Gupta, H. I. Ciftci, M. Fujita, M. Otsuka and H. R. Nasiri, *Lett. Drug Des. Discovery*, 2017, **14**, 647–661.

34 H. Yildirim, N. Bayrak, A. F. Tuyun, E. M. Kara, B. O. Celik and G. K. Gupta, *RSC Adv.*, 2017, **7**, 25753–25764.

35 E. Mataraci-Kara, N. Bayrak, H. Yildirim, M. Yildiz, M. Ataman, B. Ozbek-Celik and A. F. Tuyun, *Med. Chem. Res.*, 2021, **30**, 1728–1737.

36 N. Bayrak, M. Yildiz, H. Yildirim, E. M. Kara, B. O. Celik and A. F. Tuyun, *J. Mol. Struct.*, 2020, **1219**, 128560.

37 E. M. Kara, N. Bayrak, H. Yildirim, M. Yildiz, B. O. Celik and A. F. Tuyun, *Folia Microbiol.*, 2020, **65**, 785–795.

38 H. I. Ciftci, N. Bayrak, M. Yıldız, H. Yıldırım, B. Sever, H. Tateishi, M. Otsuka, M. Fujita and A. F. Tuyun, *Bioorg. Chem.*, 2021, **114**, 105160.

39 E. Mataraci-Kara, N. Bayrak, M. Yildiz, H. Yildirim, B. Ozbek-Celik and A. F. Tuyun, *Drug Dev. Res.*, 2021, **83**(3), 628–636.

40 C. M. Petit and K. K. Koretke, *Biochem. J.*, 2002, **363**, 825–831.

41 T. A. Keating, J. V. Newman, N. B. Olivier, L. G. Otterson, B. Andrews, P. A. Boriack-Sjodin, J. N. Breen, P. Doig, J. Dumas, E. Gangl, O. M. Green, S. Y. Guler, M. F. Hentemann, D. Joseph-McCarthy, S. Kawatkar, A. Kutschke, J. T. Loch, A. R. McKenzie, S. Pradeepan, S. Prasad and G. Martínez-Botella, *ACS Chem. Biol.*, 2012, **7**, 1866–1872.

42 S. Keinan, W. D. Paquette, J. J. Skoko, D. N. Beratan, W. Yang, S. Shinde, P. A. Johnston, J. S. Lazo and P. Wipf, *Org. Biomol. Chem.*, 2008, **6**, 3256–3263.

43 C. Acar, G. Yalçın, T. Ertan-Bolelli, F. Kaynak Onurdağ, S. Ökten, F. Şener and İ. Yıldız, *Bioorg. Chem.*, 2020, **94**, 103368.

44 M. Cerone, E. Uliassi, F. Prati, G. U. Ebiloma, L. Lemgruber, C. Bergamini, D. G. Watson, T. D. M. Ferreira, G. S. H. R. Cardoso, L. A. S. Romeiro, H. P. de Koning and M. L. Bolognesi, *Chemmedchem*, 2019, **14**, 621–635.

45 C. Ibis, A. F. Tuyun, Z. Ozsoy-Gunes, H. Bahar, M. V. Stasevych, R. Y. Musyanovych, O. Komarovska-Porokhnyavets and V. Novikov, *Eur. J. Med. Chem.*, 2011, **46**, 5861–5867.

46 Clinical and Laboratory Standards Institute (CLSI), *Performance Standards for Antimicrobial Susceptibility Testing, Clinical and Laboratory Standards Institute*, 950 West Valley Road, Suite 2500, Wayne, Pennsylvania 19087, USA, 2020.

47 Clinical and Laboratory Standards Institute (CLSI), *Reference Method for Broth Dilution Antifungal Susceptibility Testing of Yeasts; Approved Standard-Second Edition*, Wayne, PA, USA, 1997.

48 K. Yilancioglu, Z. B. Weinstein, C. Meydan, A. Akhmetov, I. Toprak, A. Durmaz, I. Iossifov, H. Kazan, F. P. Roth and M. Cokol, *J. Chem. Inf. Model.*, 2014, **54**, 2286–2293.

49 E. Mataraci-Kara and B. Ozbek-Celik, *J. Chemother.*, 2018, **30**, 82–88.

50 R. Mishra, A. K. Panda, S. De Mandal, M. Shakeel, S. S. Bisht and J. Khan, *Front. Microbiol.*, 2020, **11**, 566325.

51 R. Roy, M. Tiwari, G. Donelli and V. Tiwari, *Virulence*, 2018, **9**, 522–554.

52 J. W. Costerton, Z. Lewandowski, D. E. Caldwell, D. R. Korber and H. M. Lappin-Scott, *Annu. Rev. Microbiol.*, 1995, **49**, 711–745.

53 J. Sun, P.-C. Lv, Y. Yin, R.-J. Yuan, J. Ma and H.-L. Zhu, *PLoS One*, 2013, **8**, e69751.

54 T. Khan, K. Sankhe, V. Suvarna, A. Sherje, K. Patel and B. Dravyakar, *Biomed. Pharmacother.*, 2018, **103**, 923–938.

55 S. J. Teague, A. M. Davis, P. D. Leeson and T. Oprea, *Angew. Chem., Int. Ed. Engl.*, 1999, **38**, 3743–3748.

56 C. A. Lipinski, F. Lombardo, B. W. Dominy and P. J. Feeney, *Adv. Drug Delivery Rev.*, 2001, **46**, 3–26.

57 A. K. Ghose, V. N. Viswanadhan and J. J. Wendoloski, *J. Comb. Chem.*, 1999, **1**, 55–68.

58 D. F. Veber, S. R. Johnson, H.-Y. Cheng, B. R. Smith, K. W. Ward and K. D. Kopple, *J. Med. Chem.*, 2002, **45**, 2615–2623.

59 W. J. Egan, K. M. Merz Jr and J. J. Baldwin, *J. Med. Chem.*, 2000, **43**, 3867–3877.

60 I. Muegge, S. L. Heald and D. Brittelli, *J. Med. Chem.*, 2001, **44**, 1841–1846.

61 J. S. Delaney, *J. Chem. Inf. Comput. Sci.*, 2004, **44**, 1000–1005.

62 Y. C. Martin, *J. Med. Chem.*, 2005, **48**, 3164–3170.

63 Bruker, *APEX2, version 2014.1-1*, Bruker AXS Inc., Madison, WI, 2014.

64 Bruker, *SAINT, version 8.34A*, Bruker AXS Inc., Madison, WI, 2013.

65 Bruker, *SADABS, version 2012/2*, Bruker AXS Inc., Madison, WI, 2012.

66 Bruker, *SHELXTL, version 6.14*, Bruker AXS Inc., Madison, WI, 2000.

67 A. L. Spek, *Acta Crystallogr., Sect. D: Biol. Crystallogr.*, 2009, **65**, 148–155.

68 C. F. Macrae, P. R. Edgington, P. McCabe, E. Pidcock, G. P. Shields, R. Taylor, M. Towler and J. van De Streek, *J. Appl. Crystallogr.*, 2006, **39**, 453–457.

69 H. Tateishi, M. Tateishi, M. O. Radwan, T. Masunaga, K. Kawatashiro, Y. Oba, M. Oyama, N. Inoue-Kitahashi, M. Fujita, Y. Okamoto and M. Otsuka, *Chem. Pharm. Bull.*, 2021, **69**, 1123–1130.

70 M. O. Radwan, D. Takaya, R. Koga, K. Iwamaru, H. Tateishi, T. F. S. Ali, A. Takaori-Kondo, M. Otsuka, T. Honma and M. Fujita, *Bioorg. Med. Chem.*, 2020, **28**, 115409.

71 D. Mingle, M. Ospanov, M. O. Radwan, N. Ashpole, M. Otsuka, S. A. Ross, L. A. Walker, A. G. Shilabin and M. A. Ibrahim, *Med. Chem. Res.*, 2021, **30**, 98–108.

72 A. Daina, O. Michielin and V. Zoete, *Sci. Rep.*, 2017, **7**, 42717.